

phys. stat. sol. (b) **223**, 459 (2001)

Subject classification: 61.48.+c; 62.50.+p; 63.20.Dj; 78.30.Na; S5

High-Pressure Effects in Hydrofullerene C₆₀H₃₆ Studied by Raman Spectroscopy

K. P. MELETOV (a, b), I. TSILIKA (a), S. ASSIMOPOULOS (a), G. A. KOUROUKLIS (a), S. VES¹ (c), I. O. BASHKIN (b), V. I. KULAKOV (b), and S. S. KHASANOV (b)

(a) *Physics Division, School of Technology, Aristotle University of Thessaloniki, GR-540 06 Thessaloniki, Greece*

(b) *Institute of Solid State Physics, Russian Academy of Sciences, 142432 Chernogolovka, Moscow region, Russia*

(c) *Physics Department, Aristotle University of Thessaloniki, GR-540 06 Thessaloniki, Greece*

(Received October 4, 2000)

The effect of hydrostatic pressure on the Raman spectrum of hydrofullerene C₆₀H₃₆, at room temperature has been investigated up to 12 GPa. The samples were synthesized by means of high-pressure hydrogenation. The pressure dependence of the phonon frequencies exhibits two reversible changes one at ~0.6 GPa and another one at ~6 GPa. The first may be probably related to a phase transition from the initial orientationally disordered bcc structure to an orientationally ordered one. The second one, at ~6 GPa, is probably driven by pressure-induced bonding of hydrogen to a carbon atom of a neighboring hydrofullerene cage.

Introduction Hydrofullerenes have recently attracted considerable interest, particularly in relation to their potential use as hydrogen [1] storage materials. Several hydrofullerenes have been predicted by theoretical studies [2–4] and the synthesis of some of them, in sufficient amounts have already been reported [5, 6]. The most stable among hydrofullerenes, the C₆₀H₃₆, has been studied by various experimental methods, such as IR and Raman [7], NMR [8], UV [9, 10], X-ray emission/absorption [11] and electron/X-ray [12]/neutron diffraction [13], to identify its molecular structure and properties. The C₆₀H₃₆ molecule could exist in a great number of isomeric forms, estimated to be more than 10¹⁴ but only a small number of them may be considered to be stable [4, 10]. The isomeric form with the highest symmetry T_h has twelve double bonds, arranged as far apart as possible on its surface, while the form having the double bonds in four isolated aromatic six-membered rings lacking hydrogen atoms and located at the corners of a tetrahedron has a T symmetry structure. Between these two extremes are the isomers with symmetry D_{3d} and S₆, which have two aromatic-six membered rings at the threefold axis poles of the molecule, with the other six double bonds isolated in six pentagons. The presence of the various isomers in C₆₀H₃₆ sample depends mostly on the preparation method and on the kinetic parameters controlling the hydrogen addition reaction. Thus, C₆₀H₃₆ prepared by transfer hydrogenation of C₆₀ contains a mixture of the principal isomers D_{3d} and S₆ [7, 14], while C₆₀H₃₆, prepared by zinc reduc-

¹) Tel.: ++ (3031) 998034; Fax: (3031) 998019; e-mail: ves@auth.gr

tion of C_{60} in aromatic solvents [15], contains the S_6 isomer as the most abundant [7]. Finally, in $C_{60}H_{36}$ prepared by high pressure hydrogenation, Bini et al. [7] proposed the D_{3d} isomer as dominant, while Meletov et al. [16] proposed a mixture of D_{3d} and S_6 isomers as the most abundant. Concerning the solid-state phase of $C_{60}H_{36}$ Hall et al. [12] have suggested the body-centered cubic structure (bcc) with cell constant (11.785 ± 0.015) Å for the packing of the molecules in the crystalline state. Furthermore, they claim, at least for the D_{3d} isomer, that at sufficient low temperatures the bcc crystal structure would be transformed to a body-centered tetragonal one.

In this paper, we present the results of a micro-Raman high-pressure study of the hydrofullerene $C_{60}H_{36}$, prepared by high-pressure hydrogenation. The motivation of the present work was to study the effect of high pressure on the phonon frequencies and therefore acquire information on the structural and chemical stability of the hydrofullerene solid. The presence of hydrogen in the molecular cage may play an important role in the high-pressure behavior and on the stability region of the initial bcc phase, especially in the regime where the intermolecular and intramolecular distances become comparable. It seems interesting also to explore high pressure induced phase transition of rotational disorder/order nature in analogy to the cases of C_{60} [17], and C_{70} [18], where the phase transition from the fully orientationally disordered fcc phase to the partially/completely orientationally ordered (sc) or rhombohedral (rh) can be induced either by lowering the temperature or by increasing pressure, respectively. The prospect of hydrogen belonging to a C_{60} cage and being at the same distance from a nearby cage would produce interesting effects on the C–H vibrations as well as on the structure of the solid.

Experimental Details The starting commercial material, C_{60} of 99.99% purity, sublimated twice in a vacuum better than 10^{-5} Torr at 800 K, was compacted into pellets of 12 mm diameter and 1 mm thickness. Each pellet was placed into a copper capsule, covered with a disc of 0.01 mm thick Pd foil, and then annealed in vacuum at 620 K for 2 h to eliminate contamination with ambient gases, which could have been dissolved during compacting. The space remaining in the capsule was filled with AlH_3 and the capsule was tightly plugged with a copper lid using gallium as solder. Since both Cu and Ga are largely impermeable to hydrogen, the encapsulation described effectively prevents hydrogen losses during subsequent treatment.

The assembled capsules were pressurized to 3.0 GPa in a toroid-type high-pressure chamber and maintained at (650 ± 10) or (700 ± 10) K for a time of 24 or 48 h. The AlH_3 decomposes above 400 K [19], and the evolved hydrogen reacted with fullerite after permeating through the Pd foil, which isolated the fullerite from the chemically active Al. The amount of hydrogen gas inside the capsule corresponded to a ratio of $H/C_{60} \approx 90$ and therefore hydrogen was always in excess during the synthesis. The hydrogenation procedure was repeated a second time on the material from the run. Preliminary mass-spectroscopy data showed that at least 95% of material in ampoule is related to hydrofullerene $C_{60}H_{36}$. The rest 5% of material are partially hydrogenated fullerenes with different content of hydrogen. The X-ray analysis showed that the material has a bcc structure with a lattice parameter of 11.83 Å.

For Raman measurements visually uniform colorless or slightly yellow colored transparent specimens were chosen and placed into a Mao-Bell type high pressure cell [20]. Raman spectra were recorded using a triple monochromator (DILOR XY-500)

equipped with a liquid-nitrogen cooled CCD detector system. The spectral resolution of the system was $\sim 2 \text{ cm}^{-1}$. The 676.4 nm line of a Kr^+ laser was used for excitation, whose photon energy is located well below the fundamental absorption gap of the material. The laser power was varied from 5 to 10 mW measured directly in front of the cell. We found that at such laser powers the samples remained stable under laser irradiation for many days. The increase of the laser power to higher levels led sometimes to the destruction of samples. The 4 : 1 methanol–ethanol mixture was used as pressure transmitting medium and the ruby fluorescence technique was used for pressure calibration [21]. The phonon frequencies were determined by fitting Gaussian line shapes to the experimental Raman spectra of the hydrofullerene.

Results and Discussion Typical Raman spectra of $C_{60}H_{36}$ recorded at room temperature in the regions 100 to 800 and 1400 to 1750 cm^{-1} are shown in Fig. 1a and b for increasing and decreasing pressure, respectively. The spectral region, where the strong diamond Raman line is located, is excluded. The Raman modes appearing in the low frequency region come from the vibrations of the molecular cage and the C–H bending vibrations. As can be seen from Fig. 1 the Raman spectrum of the material is very rich with well defined structures in the low frequency region, which can easily be followed with pressure. On the contrary, the structures in the spectral region 1400 to 1750 cm^{-1} are broad and weak, but still they can be traced up to 12 GPa, the highest pressure studied. At first glance, the application of pressure seems to have the expected effect in the Raman spectrum, i.e. an overall positive shift in the frequencies of the Raman modes and a relative increase in their line widths. However, the situation is

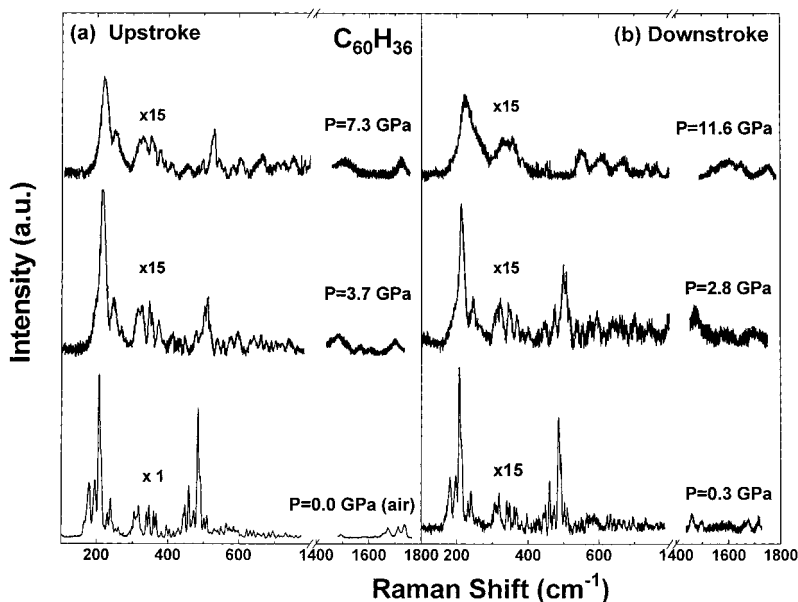


Fig. 1. Raman spectra of $C_{60}H_{36}$ recorded at room temperature during a) increasing and b) decreasing pressure cycle in the frequency region 100–1800 cm^{-1} . The frequency region containing the strong diamond Raman line is excluded

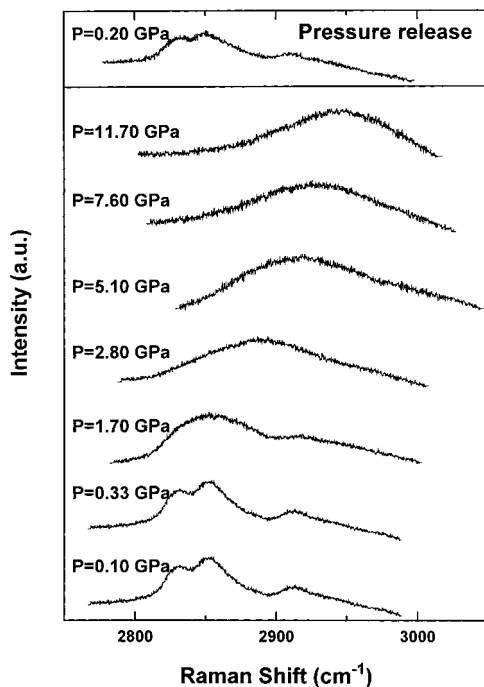


Fig. 2. Raman spectra of $C_{60}H_{36}$ recorded in the frequency region of C–H stretching mode at ambient temperature and various pressures. In the upper part the spectrum at 0.2 GPa is recorded upon pressure release

changed dramatically for the part of the Raman spectrum between 2800 and 3000 cm^{-1} containing the hydrogen stretching vibrations. As can be seen in Fig. 2, where the C–H stretching vibration frequency region is depicted, the initially well-separated structures that are seen up to 1.7 GPa are gradually washed out into a very broad structure for pressures higher than 2.0 GPa. The pressure effect on the Raman spectrum is fully reversible upon releasing pressure as shown in Fig. 1 and the top part of Fig. 2.

The effect of C_{60} hydrogenation makes its presence clear by the dramatic changes in the Raman spectrum. A remarkable increase in the number of the Raman active modes is observed in comparison to C_{60} .

This would be expected by the lowering of the symmetry due to the hydrogenation and to the formation of new bonds. In addition to the C–H stretching modes, new modes related to the C–H bending vibrations appear in the frequency region 1150–1350 cm^{-1} [16] the pressure evolution of the new modes could not be followed because first, they are partly obscured by the very strong diamond Raman line and second, they become broad very quickly with increasing pressure. The expected number of Raman active modes depends strongly on the symmetry of the isomer. Taking into consideration the most stable isomers of $C_{60}H_{36}$ and by using standard group theoretical arguments, one can show that the expected Raman active modes are 118, 60, 73 and 95 for the T_h , T_h , D_{3d} and S_6 isomers, respectively. The number of recorded lines at ambient pressure is at least 126, which points to the fact that the samples under investigation do consist of a mixture of at least two major isomers. A detailed study of the recorded Raman lines [16] and comparison with theoretical estimations [7], indicate that they contain all five of the lowest free energy isomers, and those with symmetry D_{3d} and S_6 are the most abundant.

In Figs. 3 and 4 we present the pressure dependence of the well-resolved Raman lines as a function of pressure at room temperature. The open (closed) symbols correspond to pressure increase (decrease), while the solid lines through the experimental points represent linear least squares fittings. Different symbols correspond to different runs. The shaded areas near $P \sim 0.6$ and ~ 6.0 GPa denote the change in the slope of the pressure induced frequency shift, or the disappearance of some Raman lines. The fitting parameters and a tentative mode assignment of the observed modes are com-

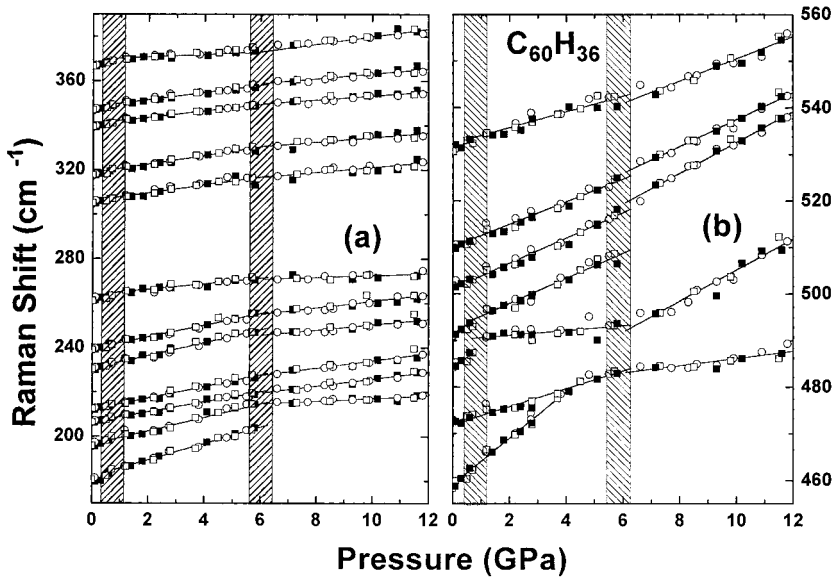


Fig. 3. Pressure dependence of low frequency Raman active modes of $C_{60}H_{36}$ in the frequency regions, a) $150\text{--}400\text{ cm}^{-1}$ and b) $450\text{--}560\text{ cm}^{-1}$. The peak positions are obtained by fitting Gaussians to the experimental data. Open (closed) symbols correspond to increasing (decreasing) pressure. Solid lines represent linear least squares fits. The different symbols correspond to different pressure runs. The shaded areas at $P \sim 0.6$ and ~ 6.0 GPa denote the regions in which changes in the slope of the pressure dependence and disappearance of several Raman lines are observed

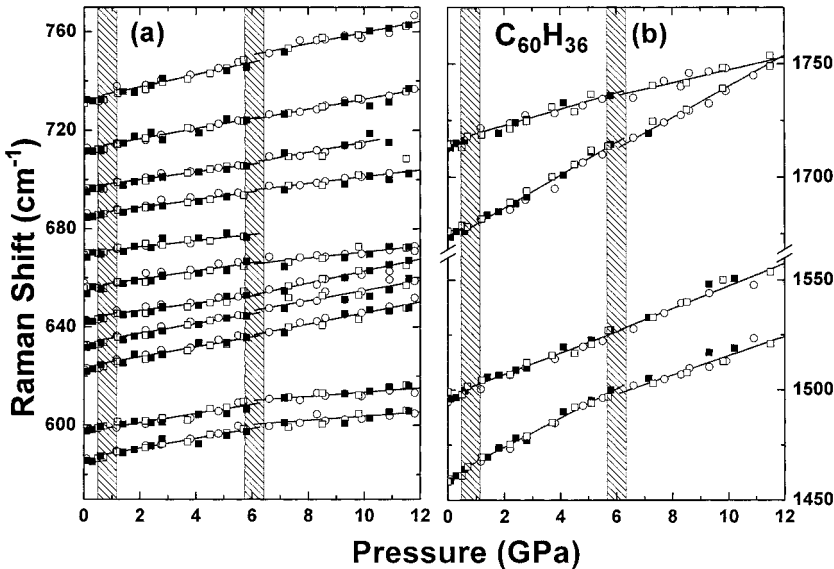


Fig. 4. The same as in Fig. 3, but in the frequency regions a) $570\text{--}770\text{ cm}^{-1}$ and b) in the region $1450\text{--}1750\text{ cm}^{-1}$

piled in Table 1. In the mode assignment column we indicate the isomeric form to which this mode most likely belongs. The mode assignment is based on the theoretical predictions by Bini et al. [7]. Also for comparison the corresponding data for C_{60} are included. From Figs. 3 and 4 and Table 1 we see that all the observed modes have positive pressure coefficients and at least four lines disappear for pressures higher than 6 GPa. Furthermore, the majority of them exhibit a reversible change in the slope of their pressure dependence at 0.6 and 6 GPa.

In the absence of any structural investigations of $C_{60}H_{36}$ under pressure we try to understand the observed behavior of the Raman lines with pressure by comparing the

Table 1

The phonon frequencies, their assignment and the pressure coefficients for the $C_{60}H_{36}$ Raman active modes. The corresponding values for C_{60} are also included for comparison

Mode	$\omega (P = 0)$ (cm^{-1})	$C_{60}H_{36}$			C_{60} ^{a)}	
		0–0.7 GPa	1.16–5.8 GPa	6.6–11.8 GPa	0.4–2.4 GPa	
		$\partial\omega_i/\partial P$ ($\text{cm}^{-1}/\text{GPa}$)	$\partial\omega_i/\partial P$ ($\text{cm}^{-1}/\text{GPa}$)	$\partial\omega_i/\partial P$ ($\text{cm}^{-1}/\text{GPa}$)	ω (cm^{-1})	$\partial\omega_i/\partial P$ ($\text{cm}^{-1}/\text{GPa}$)
$T_g(T)$	180.6	5.6 ± 0.1	6.4 ± 0.1			
$E_g(T_h)$	196.0	4.7 ± 0.6	3.1 ± 0.4	0.6 ± 0.1		
$E_g(T)$	206.6	2.7 ± 0.3	2.2 ± 0.1	1.6 ± 0.1		
$T_g(T_h)$	212.6	2.3 ± 0.3	2.6 ± 0.1	1.7 ± 0.2		
$E_g(D_{3d})$	230.6	3.5 ± 0.1	2.9 ± 0.1	1.2 ± 0.2		
	239.1	3.2 ± 0.2	2.6 ± 0.2	1.5 ± 0.2		
	261.1	2.1 ± 0.1	1.3 ± 0.1	0.4 ± 0.2	272 $H_g(1)$	3.2
	305.2	2.2 ± 0.2	1.8 ± 0.2	1.2 ± 0.2	294 ω_1	2.5
	317.8	3.1 ± 0.1	1.9 ± 0.1	1.0 ± 0.2		
$E_g(D_{3d})$	339.6	2.1 ± 0.1	1.4 ± 0.1	0.9 ± 0.1		
$A(S_6)$	347.1	2.8 ± 0.1	1.6 ± 0.1	1.1 ± 0.1	345 ω_2	2.9
$E_g(T_h)$	366.7	3.2 ± 0.2	0.6 ± 0.2	1.7 ± 0.3		
$A_g(S_6)$	458.7	5.2 ± 1.2	4.6 ± 0.3		454 ω_4	1.4
	472.4	2.0 ± 0.8	1.9 ± 0.2	0.8 ± 0.1		
$A_g(T)$	484.2	4.6 ± 0.2	0.5 ± 0.2	3.3 ± 0.2		
$A_g(S_6)$	491.0	3.3 ± 0.1	2.7 ± 0.1		495 $H_g(2)$	4.2
	501.8	2.0 ± 0.1	2.7 ± 0.1	3.3 ± 0.1		
$E_g(S_6)$	530.6	2.7 ± 0.2	1.7 ± 0.2	2.4 ± 0.2	522 ω_5	1.0
$E_g(D_{3d})$	585.7	2.6 ± 0.2	2.0 ± 0.2	0.8 ± 0.2		
$E_g(S_6)$	598.6	2.3 ± 0.2	1.9 ± 0.2	0.9 ± 0.2		
$T_g(T_h)$	622.6	2.9 ± 0.2	2.0 ± 0.2	2.3 ± 0.2	624 ω_7	1.5
$E_g(D_{3d})$	632.5	2.4 ± 0.1	2.0 ± 0.1	2.0 ± 0.3		
$E_g(D_{3d})$	642.5	2.0 ± 0.2	1.5 ± 0.2	2.5 ± 0.2		
$T_g(T)$	655.8	1.2 ± 0.2	1.7 ± 0.2	1.2 ± 0.2		
$E_g(T_h)$	669.3	1.9 ± 0.1	1.3 ± 0.1			
$A_{1g}(D_{3d})$	695.6	1.8 ± 0.1	1.6 ± 0.1	2.0 ± 0.4		
$A_{1g}(D_{3d})$	730.9	1.4 ± 0.2	2.5 ± 0.2	2.3 ± 0.2	729 ω_8	-2.9
$T_g(T)$	1459.5	10.0 ± 0.2	6.7 ± 0.2	4.4 ± 0.4	1467 $A_g(2)$	5.5
$E_g(S_6) ?$	1494.5	9.6 ± 0.3	4.8 ± 0.3	5.1 ± 0.4		
$A_g(S_6)$	1674.6	4.6 ± 0.3	7.2 ± 0.3	6.9 ± 0.4		
$A_g(T_h)$	1712.5	5.2 ± 0.3	3.6 ± 0.3	2.8 ± 0.5		

^{a)} Data taken from K. P. Meletov, G. A. Kourouklis, D. Christophilos, and S. Ves, Zh. Eksper. Theor. Fiz. **108**, 1456 (1995) [J. Exper. Theor. Phys. **81**, 798 (1995)].

corresponding behavior of C_{60} and C_{70} . For example, at 0.4 GPa at room temperature [17] or by cooling down to 259 K, C_{60} transforms from the fcc structure, in which the C_{60} rotation are completely disordered, to the sc structure, where the molecular rotations are partially ordered. Similarly, C_{70} [18] undergoes an orientational ordering phase transition from an fcc structure to a rhombohedral phase at 0.35 GPa or by cooling at 280 K. Furthermore, Hall et al. [12] found that the distortion of the molecules brought about by the hydrogenation together with the hydrogen atoms around the equator gives to the $C_{60}H_{36}$ molecule a strongly oblate shape. The bcc structure allows effective packing of oblate spheroids if the polar axes of the molecules are aligned. The longer second-nearest neighbor distance then prevents close approaches of the equatorial hydrogen atoms. If this alignment really occurs, then there should be a tendency to form a tetragonal structure with c/a less than unity. So they predict that at sufficiently low temperatures the bcc structure will transform to a body-centered tetragonal structure. Thus, keeping in mind the pressure behavior of C_{60} and C_{70} and the finding by Hall et al. [12], we speculate that the observed anomaly at 0.6 GPa in the observed Raman modes could be assigned to such a structural transition, i.e., from the bcc to a tetragonal structure. This assumption would explain in some way the observed pressure coefficient discontinuity at 0.6 GPa and the strong broadening of the hydrogen C–H stretching modes, since in the tetragonal phase the hydrogen atoms are coming closer to each other and so the enhanced interaction is expected to broaden the spectral lines.

The most striking effect of pressure on the Raman spectra of $C_{60}H_{36}$ is on the stretching C–H vibrations, where a dramatic broadening occurs with increasing pressure. This may be attributed to the enhancement of the interaction between the hydrogen atoms and the C_{60} molecular cages as the volume decreases. Although this interaction is expected to be very complicated and it will become much more so in the structural phase transition regime, we could, to a first approximation for a qualitative understanding, assume that the number of the main C–H Raman modes of $C_{60}H_{36}$ *do not change* with pressure and therefore, the observed broadening could be attributed to the variable

local fields experienced by H-bonds, especially as the intramolecular distances become comparable to the intermolecular ones. We think that this is also substantiated by our data, as the corresponding spectra are significantly broad also at ambient pressure. With this assumption in mind we have fitted the experimental data in the C–H region of the Raman spectra, by keeping the number of peaks

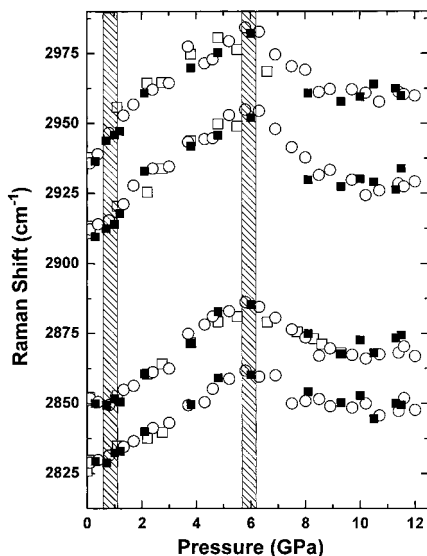


Fig. 5. Pressure dependence of the Raman active modes of $C_{60}H_{36}$ in the frequency region of the C–H stretching modes. Different symbols correspond to different experimental runs. The peak positions are obtained by fitting Gaussians to the experimental data of Fig. 2

equal to four. The pressure behavior of the peaks obtained in this way is displayed in Fig. 5. Despite the crudeness of our procedure, the pressure dependence of the C–H Raman peaks show a behavior, which, up to ~ 6 GPa, is compatible with that of the fullerene molecular cage modes. For example, an overall positive shift, up to about 6 GPa, and changes in the slopes of the pressure dependence of the mode frequencies at the same critical pressure in the low pressure regime are similar to the case of the cage modes. However, their pressure dependence is different for pressures higher than 6 GPa, where a softening in the C–H stretching vibrations is observed. We would like to mention that even if we follow the frequency of the “centre of gravity” of the C–H Raman band as a function of pressure, we find a change in the slope of the pressure dependence at about 6 GPa. Concerning the anomaly in the pressure dependence at ~ 6 GPa in the Raman spectra, especially the behavior of the C–H stretching modes, this could be attributed to a possible second phase transition in which hydrogen bonding is involved. At this pressure it is reasonable to assume that the intermolecular and intramolecular distances start becoming comparable and therefore hydrogen interaction with carbon atoms belonging to a neighboring molecular cage is enhanced. As the pressure increases further, this interaction is facilitated resulting in the softening of the C–H bonds. This phase transition is reversible as clearly indicated by our experimental data (see Fig. 2). Such a behavior of hydrogen bonds under pressure is already known in materials containing hydrogen bonds, which under pressure exhibit a softening in their vibrational frequency because of the pressure induced enhancement of the hydrogen interaction [22].

Acknowledgements The support by the General Secretariat for Research and Technology and the European Social Fund (grant #PIENEΔ99, 99EΔ/62) is gratefully acknowledged. K. P. M. acknowledges the support by the General Secretariat for Research and Technology, Greece, and the Russian Foundation for Fundamental Research (grant #99-02-17555). I. O. B. acknowledges the support by Russian Research and Development Program “Fullerenes and Atomic Clusters” (grant #98079), and the Russian Foundation for Fundamental Research (grant #99-02-17299).

References

- [1] A. C. DILLON, K. M. JONES, T. A. BEKKEDAH, C. H. KIANG, D. S. BETHUNE, and M. J. HEBEN, *Nature* **386**, 377 (1997).
- [2] A. RATHNA and J. CHANDRASEKHAR, *Chem. Phys. Lett.* **206**, 217 (1993).
- [3] L. D. BOOK and G. E. SCUSERIA, *J. Phys. Chem.* **98**, 4283 (1994).
- [4] B. I. DUNLAP, D. W. BRENNER, and G. W. SCHRIVER, *J. Phys. Chem.* **98**, 1756 (1994).
- [5] M. I. ATTALLA, A. M. VASSALLO, B. N. TAITAM, and J. HAMMA, *J. Phys. Chem.* **97**, 6329 (1993).
- [6] I. O. BASKIN, A. I. KOLESNIKOV, V. E. ANTONOV, E. G. PONYATOVSKY, A. P. KOBZEV, A. Y. MUZYCHKA, A. P. MORAVSKY, F. E. WAGNER, and G. GROSSE, *Mol. Mater.* **10**, 265 (1998).
- [7] R. BINI, J. EBENHOCH, M. FANTI, P. W. FOWLER, S. LEACH, G. ORLANDI, CH. RÜCHARDT, J. P. B. SANDALL, and F. ZERBETTO, *Chem. Phys.* **232**, 75 (1998).
- [8] W. E. BILLUPS, A. GONZALEZ, C. GESENBERG, W. LUO, T. MARRIOT, L. B. ALEMANY, M. SAUNDERS, H. A. JIMENEZ-VAZQUENZ, and A. KHONG, *Tetrahedron Lett.* **38**, 175 (1997).
- [9] A. GOVINDARAJ, *Curr. Sci.* **65**, 868 (1993).
- [10] M. BÜHL, W. THIEL, and U. SCHNEIDER, *J. Amer. Soc.* **117**, 4623 (1995).
- [11] Y. MURAMATSU, Y. UENO, T. HAYASHI, M. M. GRUSH, E. M. GULLIKSON, and R. C. C. PERERA, *J. Electron Spectrosc. Relat. Phenom.* **107**, 177 (2000).
- [12] L. E. HALL, D. R. MCKENZIE, M. I. ATTALLA, A. M. VASSALLO, R. L. DAVIS, J. B. DUNLOP, and D. J. H. COCKAYNE, *J. Phys. Chem.* **97**, 5741 (1993).

- [13] L. E. HALL, D. R. MCKENZIE, R. L. DAVIS, M. I. ATTALLA, and A. M. VASSALLO, *Acta Cryst.* **B54**, 345 (1998).
- [14] R. V. BENSANSSON, T. J. HILL, E. J. LAND, S. LEACH, D. J. MCGARVEY, T. G. TRUSCOTT, J. EBENHOCH, M. GERST, and C. RÜCHARDT, *Chem. Phys.* **215**, 111 (1997).
- [15] A. D. DARWISH, A. K. ABDUL-SADA, G. J. LANGLEY, H. W. KROTO, R. TAYLOR, and D. R. WALTON, *J. Chem. Soc. Perkin Trans.* **2**, 2359 (1995).
- [16] K. MELETOV, S. ASSIMOPOULOS, I. TSILIKA, I. O. BASHKIN, V. I. KULAKOV, S. S. KHASANOV, and G. A. KOUROUKLIS, *Chem. Phys.* (2001), to be published.
- [17] K. P. MELETOV, G. KOUROUKLIS, D. CHRISTOFILOS, and S. VES, *Phys. Rev. B* **52**, 10090 (1995).
- [18] C. CHRISTIDES, I. M. THOMAS, T. J. DENNIS, and K. PRASSIDES, *Europhys. Lett.* **22**, 611 (1993).
A. LUNDIN, A. SOLDATOV, and B. SUNDQUIST, *Europhys. Lett.* **30**, 469 (1995).
- [19] S. K. KONOVALOV and B. M. BULYCHEV, *Zh. Neorg. Khim.* **37**, 2640 (1992).
- [20] A. JAYARAMAN, *Rev. Sci. Instrum.* **57**, 1013 (1986).
- [21] D. BARNETT, S. BLOCK, and G. J. PIERMARINI, *Rev. Sci. Instrum.* **44**, 1 (1973).
- [22] E. KATOH, H. YAMAWAKI, H. FUJIHISA, M. SALASHITA, and K. AOKI, *Phys. Rev. B* **59**, 11244 (1999).

